MICROSTRUCTURE CHARACTERIZATION IN CEMENT PASTE USING BACKSCATTERED DIFFUSE ULTRASOUND

M. Goueygou[1], J. Popovics[2], K. Hall[2], M. Oelze,[3] and Z. Lafhaj[4]

[1]Institute of Electronics, Microelectronics and Nanotechnologies, DOAE UMR CNRS 8520, Ecole Centrale de Lille, Villeneuve d'Ascq, France
[2]Department of Civil & Environmental Engineering, University of Illinois, Urbana-Champaign, USA
[3]Department of Electrical & Computer Engineering, University of Illinois, Urbana-Champaign, USA
[4]Laboratory of Mechanics, UMR CNRS 8107, Ecole Centrale de Lille, Villeneuve d'Ascq, France

ABSTRACT. In this paper, the quantitative ultrasound technique (QUS) technique is applied to characterize voids in cement paste. Experiments are conducted on two series of cement paste specimens: a pair of regular samples with two levels of capillary porosity and a pair of air entrained samples with two concentrations of bubbles. The specimens are placed in a water tank and scanned at 5 MHz in pulse-echo mode. Velocity, attenuation, transmission coefficient and backscattering cross section are measured. Then, several models are used to estimate the parameters of the microstructure from the backscattered energy. Finally, the microstructure is analyzed from digital images. In the air-entrained samples, the mean scatterer size is correctly estimated and a clear difference in the acoustic concentration is observed in both samples, although this difference is higher than expected. In regular cement paste, the ultrasonically estimated scatterer size is too high to correspond to capillary pores. In this case, the scattered energy may originate from clumps of flocculated cement paste.

Keywords: Ultrasound, Concrete, Microstructure, Backscattering, Structure Noise
PACS: 43.35.Zc

INTRODUCTION

Due to its relatively low cost, ease of workability and high mechanical strength, concrete has become the most widespread construction material. It is composed of solid phases (cement and aggregates) and air or liquid-filled voids, consisting of capillary pores, bubbles and cracks. Capillary porosity depends essentially on the water/cement (w/c) ratio and is typically between 5% and 18% in volume, with pore size ranging from the nm to the μm scale. In order to improve resistance to frost, air bubbles can be entrained using a chemical additive. Cracks, which are already present in hardened concrete at its initial state, can be further increased by mechanical loading, thermal stress or physicochemical reactions. Therefore, concrete contains a complex network of voids of various geometry and sizes. This network determines not only its mechanical strength, but also its durability, as various reactive substances may diffuse into the concrete interior through connected pores and cracks, or remain

CP1096, *Review of Quantitative Nondestructive Evaluation Vol. 28,*
edited by D. O. Thompson and D. E. Chimenti
© 2009 American Institute of Physics 978-0-7354-0629-2/09/$25.00

Downloaded 19 Jun 2009 to 130.126.119.40. Redistribution subject to AIP license or copyright; see http://proceedings.aip.org/proceedings/cpcr.jsp

trapped inside bubbles. Porosity and permeability, which describe this network at the macroscopic level, are thus considered as relevant durability indices. They are usually measured from cores extracted from the structure under study. Core sampling can be performed only to a limited extent, but it is the only way for investigating transfer properties of concrete in structures, as quantitative non-destructive methods have not yet reached a level of maturity where estimates of pore properties are reliable and robust.

For several decades, ultrasonic testing has been used for assessing integrity and characterizing properties of various materials, including concrete [1,2]. Conventional ultrasonic techniques process the coherent response to a pulsed wave to extract parameters such as velocity and attenuation, which depend on microstructure [3]. In highly heterogeneous materials, such as concrete, the coherent response tends to vanish due to wave scattering, especially as frequency and distance of propagation increase. In this case, the ultrasonic signal is mostly incoherent. Depending on the field of application, the incoherent part of the ultrasonic/acoustic signal is designated by different names: "speckle" in medical ultrasonography, "coda" in geophysics, "structure noise" in NDT, "diffuse" in acoustics. Although it has long been considered noise, the incoherent field does contain information on the medium of propagation. In medical imaging, the ultrasonic speckle has been analyzed to characterize tissue properties. The quantitative ultrasound (QUS) technique was developed by Lizzi et al. [4] and Insana et al. [5] to characterize the microstructure of biological tissues. It consists in measuring the frequency-dependent backscattering cross section (BCS), which is then fitted to an analytical model, assuming a known shape of scatterers or spatial variation of their elastic properties. The best fit yields estimates of the mean size and acoustic concentration of scatterers in the insonicated region.

In this study, the ability of the QUS technique to characterize the microstructure of cementitious materials is investigated. The samples consist of two pairs of hardened cement paste, one with two levels of capillary porosity and one with two levels of bubble concentration. For each sample, the BCS is measured from a B-scan using a 5 MHz focused transducer. Several models are then tested to fit the measured coefficient. They differ in the assumed scatterer type (localized or distributed), acoustic contrast (weak or strong scattering) and size distribution (mono or multidispersed scatterers). In the first section of this paper, the principles of the QUS technique are recalled. In the second section, the fabrication of cement paste samples and the ultrasonic experiment are described. In the third section, ultrasonic estimates of air void size and concentration are presented and compared to reference data obtained from digital images of the sample surface. Finally, conclusions are given concerning the ability of the QUS technique to characterize the microstructure of cementitious materials.

THEORY

First, the QUS technique aims at relating the average backscattered power from multiple scatterers to the backscattering cross section (BCS) of a single scatterer. The scattering cross section is defined (in $sr^{-1}.cm^{-1}$) as the ratio per unit volume of the intensity I_{scat} at distance R scattered in direction θ into a unit solid angle and the intensity I_{inc} of an incident plane wave [5] :

$$\sigma_{scat}(f,\theta) = \frac{R^2}{V}\frac{\langle I_{scat}(R,\theta)\rangle}{\langle I_{inc}\rangle} \tag{1}$$

where V is the scatterer's volume. The BCS is simply equal to the scattering cross section in the direction opposite to the incident wave, i.e. $\sigma_b(f) = \sigma_{scat}(f,\theta=\pi)$. A

Downloaded 19 Jun 2009 to 130.126.119.40. Redistribution subject to AIP license or copyright; see http://proceedings.aip.org/proceedings/cpcr.jsp

relationship between the average backscattered power and the BCS was derived by and Insana et al. [5] assuming :

i. Single scattering only.
ii. Incoherent scattering, i.e. no spatial correlation between the locations of scatterers.
iii. A quasi plane wave within the focal region of the ultrasonic beam.
iv. No shear mode in the background medium.

Under these assumptions, it can be written as :

$$\sigma_b(f) = \frac{0.36 R_1^2}{A_0 \Delta z} W_{norm}(f) \tag{2}$$

The parameters of Eq.2 correspond to the measurement geometry and are described in Fig. 1. The normalized average backscattered power (W_{norm}) is computed as :

$$W_{norm}(f) = \frac{1}{N} \sum_{i=1}^{N} \left(\frac{\gamma}{2} \right)^2 \frac{1}{T_m^2} \frac{|S_m(f, z_1)|^2}{|S_{ref}(f, z_1)|^2} AC(f) \tag{3}$$

S_m is the spectrum of the signal backscattered from the region of interest (ROI) in the test sample, S_{ref} the spectrum of the signal reflected from a reference sample (a polished 10 mm thick plexiglas plate), γ is the reflection coefficient between water and the reference sample, T_m is the transmission coefficient between water and the test sample, N_l is the number of signals in the ROI. Normalization aims at compensating for the transducer's electro-acoustic transfer function. The frequency-dependent effect of attenuation in the test sample is also compensated through function AC [6].

Once the BCS is estimated as a function of frequency, it is compared with the correlation models listed in Table 1. The weak scattering assumption (Born approximation) results in simple relationships between the BCS and scatterer parameters : scatterer radius a, number density n_v and impedance contrast γ_0. For single-sized scatterers, it leads to the fluid sphere model (*FS_B*) for discrete scatterers and to the Gaussian model for a continuous distribution of scattering properties. If the Born approximation is released,

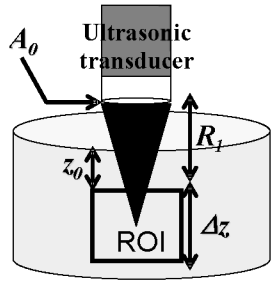

FIGURE 1. Measurement geometry for BCS estimation using the QUS technique. A_0 is the active area of the transducer.

Downloaded 19 Jun 2009 to 130.126.119.40. Redistribution subject to AIP license or copyright; see http://proceedings.aip.org/proceedings/cpcr.jsp

TABLE 1. Correlation models for estimating microstructural parameters. k is the longitudional wavenumber in the background medium, a the scatterer radius, $n_v\gamma_0^2$ the acoustic concentration, $N_v(a_i)$ the number density of scatterers around radius a_i.

	Single size	Size distribution
Weak scattering	*Fluid Sphere (FS_B)* $\sigma_b(f)=\frac{k^4a^6}{9}n_v\gamma_0^2\left(3\frac{j_1(2ka)}{2ka}\right)^2$ [5]	*Distributed Fluid Spheres (DFS_E)* $\sigma_b(f)=\sum_i N_v(a_i)\sigma_b(f,a_i)$ [8]
	Gaussian $\sigma_b(f)=\frac{k^4a^6}{9}n_v\gamma_0^2e^{-2k^2a^2}, 2a_{eff}\cong 3.11d$ [5]	
Full solution	*Single Fluid Sphere (SFS_E)* $\sigma_b(f)=\left\lvert\frac{j}{2k}\sum_{m=0}^{+\infty}(2m+1)\{1+R_m(ka)\}P_m(-1)\right\rvert^2$ [7]	

TABLE 2. Characteristics of test specimens. %AE is the percentage weight of air-entrainer relative to the cement weight.

	CP1	CP2	AE1	AE2
w/c	0,3	0,6	0,5	0,5
%AE	0	0	0,05	0,2
density (kg/m^3)	2000	1820	1450	1350

the single-sized exact fluid sphere model (*SFS_E*) is obtained. This model can be further generalized to account for the size distribution (*DFS_E*). In our case, the scatterers (pores, air voids and bubbles) are assumed to be filled with air or water, so we have $\gamma_0 \approx 1$. The two other unknowns (a and n_v) are then estimated by minimizing the mean square distance between the measured and model BCS.

EXPERIMENTS

Test Specimens

The test specimens consist in two pairs of cement paste slices : one pair of regular cement paste samples (CP1 & CP2) with different water/cement ratios (w/c) and one pair of air-entrained samples (AE1 & AE2) with different bubble concentrations. Components and characteristics of the specimens are given in Table 2. Cement and water are mixed for about 3 min using a low speed kitchen mixer, except for AE2 where the mixing time and speed are increased up to 20 min to enhance bubble formation. The mix is then cast into a 10×4" cylindrical mold. In order to minimize air voids in the CP1 and CP2 batches, the molds are placed in a sealed glass container and manually shaken while air is pumped out from the container. The cylinders are then cured for 28 days in a moist room. After curing, two slices are cut for each batch at the center of the cylinder, a thick one (2" thick) for the QUS measurement and a thin one (0,5" thick) for other ultrasonic measurements and image analysis. To allow for uniform saturation conditions, all slices are kept for 2 weeks in water saturated with lime before ultrasonic measurement are made.

Ultrasonic Measurements

For each specimen, the QUS measurement consists in a single line scan along the specimen's diameter using a 5 MHz F4 transducer (0,5" ∅, 2" geometrical focal length, λ≈800 μm). The transducer is connected to a Panametrics© 5800 pulser-receiver and set

Downloaded 19 Jun 2009 to 130.126.119.40. Redistribution subject to AIP license or copyright; see http://proceedings.aip.org/proceedings/cpcr.jsp

on a Daedal© micro-positioning system with 3 translational and 2 rotational axes. The specimen is placed at the bottom of a tank filled with degassed water. The transducer focus is placed 3 mm below the specimen's surface. The spatial step of the scan is set approximately to the -6 dB beamwidth at the focus (1,2 mm). The reference signal (S_{ref} in Eq.3) is obtained by averaging signals from a 30 mm long axial scan around the focus. In order to normalize the backscattered power, coherent parameters (pulse velocity, attenuation and transmission coefficient) are measured in pulse-echo on the thin slice using the buffer rod method [9]. For each scan, values of the BCS are estimated from eight 1×1 cm^2 ROIs within the -12 dB bandwidth of the reference signal.

Image Analysis

In order to assess the ultrasonic estimates of micro-structural parameters (size and percentage volume), the geometry of the structures visible on the specimen surface is analyzed. To enhance the contrast between voids and background, the polished surface of each specimen is first dyed using a black marker, then the voids are filled with a thin white powder (gypsum) and the excess powder is eliminated using a thin edge. A digital picture of the surface is taken with pixel size around 50 µm. The pictures are analyzed using a Matlab© script and the Image Analysis Toolbox©. The script converts the picture into a binary file, identifies groups of white connected pixel corresponding to voids, yields the apparent fraction (p_A) , number density (n_A) and – assuming those void are spherical - the apparent diameter distribution (d_A). Using stereological principles [10], those results can be extrapolated to estimate volumetric features :

$$\text{Volume/area fraction :} \quad p_V = p_A \tag{4a}$$

$$\text{Real/apparent mean diameter :} \quad \langle D_V \rangle = \frac{\pi}{2} H(d_A) \tag{4b}$$

$$\text{Volume/area number density :} \quad n_V = n_A / \langle D_V \rangle \tag{4c}$$

In these equations, subscript A refers to the apparent (or area) parameter and subscript V to the real (or volumetric) parameter.

RESULTS

For the four specimens, the values of measured coherent parameters are presented in Fig. 2. Error bars are not shown on the attenuation graph (Fig. 2.b) since it was estimated from single averaged front-wall and back-wall signals. Going from CP1 to AE2, a decrease of pulse velocity (Fig. 2.a) and an increase of transmission coefficient (Fig. 2.c) are observed. This is explained by the increasing number of voids – thus decreasing specimen's stiffness – and the decreasing density – thus decreasing specimen's acoustic impedance. The increase of attenuation coefficient (Fig. 2.b) is related to the increasing heterogeneity and scattering of the specimen.

The fit of the experimental BCS (σ_{meas}) with the model (σ_{model}) is assessed using a generalized regression coefficient [11] :

Downloaded 19 Jun 2009 to 130.126.119.40. Redistribution subject to AIP license or copyright; see http://proceedings.aip.org/proceedings/cpcr.jsp

$$R^2 = 1 - \frac{\left\langle \left(\sigma_{meas} - \sigma_{model} \right) \right\rangle}{var\left(\sigma_{meas} \right)} \tag{5}$$

In this formula, the mean and variance are calculated over frequencies. The R^2 values for each specimen and model are given in Fig. 3. For the "CP" specimens, a good fit ($R^2 > 0{,}8$) is obtained for the weak scattering models (Gaussian and FS_B). For the air-entrained specimens (AE), the quality of the fit is significantly degraded. Only the full solution for distributed scatterer size (DFS_E) yields $R^2 > 0{,}5$. This may be due to the fact that the background medium in the AE specimens is not homogeneous at the wavelength scale. Besides the bubbles, weaker scatterers, such as clumps of flocculated cement grains, may be present in large quantities and contribute significantly to ultrasonic scattering. However, all the models used consider that scatterers are filled with the same material, i.e. water, and cannot account for different types of scatterers. Note also the poor performance of the exact, single sized model (SFS_E), which suggest that the size distribution of scatterers is not monodispersed. The microstructural parameters obtained by the QUS technique are presented in Fig. 4 and compared with the results of image analysis (IA). The weak scattering models (Fig. 4.a and 4.b) give a reasonable estimate of the scatterer size - around 250 μm for all samples – but largely overestimates their concentration. On the other hand, the models based on the full solution (Fig. 4.c and 4.d) underestimate the scatterer size, but yield the right order of magnitude for their concentration (n_v<10%). Surprisingly, the AE1 specimen is found to have the lowest void concentration, according to the QUS result. Several authors [8] have already observed the high variance and inaccuracy of this index. In addition, image analysis gives only a partial view of the microstructure : only the larger voids (> 50 μm) are observed, and clumps of cement grains or other variations of properties are not visualized. Other techniques, such as Mercury Intrusion Porosimetry (MIP), optical or scanning electron microscopy, should be utilized as a reference measurement to characterize the cement paste microstructure more accurately.

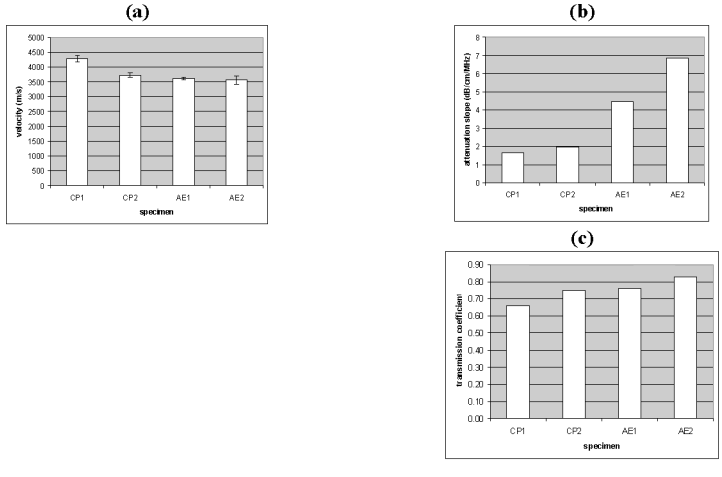

FIGURE 2. Measured coherent parameters. a. Pulse velocity; b. Attenuation slope; c. water-to-specimen transmission coefficient.

Downloaded 19 Jun 2009 to 130.126.119.40. Redistribution subject to AIP license or copyright; see http://proceedings.aip.org/proceedings/cpcr.jsp

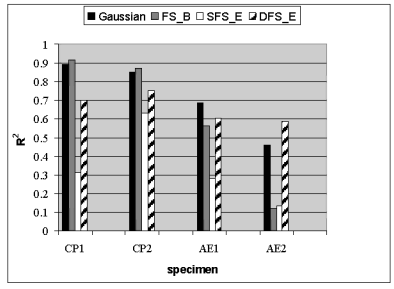

FIGURE 3. R^2 values (Eq.5) for all four models and specimens.

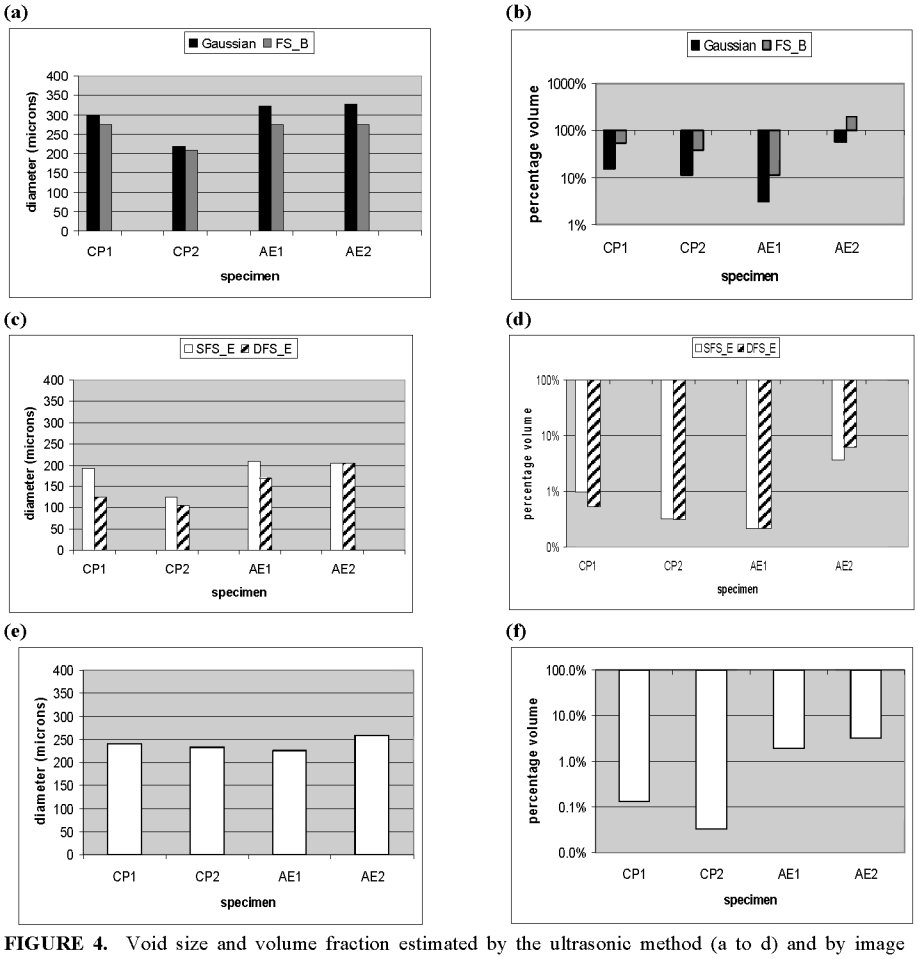

FIGURE 4. Void size and volume fraction estimated by the ultrasonic method (a to d) and by image analysis (e and f). Section a and b correspond to weak scattering models (FS_B and Gaussian) , section c and d to the full solution (SFS_E and DFS_E).

Downloaded 19 Jun 2009 to 130.126.119.40. Redistribution subject to AIP license or copyright; see http://proceedings.aip.org/proceedings/cpcr.jsp

CONCLUSIONS

This paper describes an attempt to estimate microstructural parameters (void size and concentration) in cement paste using high-frequency diffuse ultrasound. The technique is based on a quantitative estimate of the backscattering cross section of a single scatterer and a fit with different analytical models. The weak scattering models yields reasonable estimates of the void size. The models based on the full solution give the right order of magnitude for the void concentration. The discrepancy between the ultrasonic result and reference data obtained by image analysis may be related to the presence of scattering structures (clumps of cement grains) that are not visible on the image. The simple assumption of a single type of scatterer (water or air filled voids) may also be questioned. Future work will require using more accurate techniques to characterize the microstructure of cement paste at a smaller scale.

ACKNOWLEDGEMENTS

M. Goueygou is grateful to the Fullbright Foundation, the Nord-Pas-de-Calais region and Ecole Centrale de Lille for supporting his stay at the University of Illinois at Urbana-Champaign.

REFERENCES

1. Popovics, J.S., Rose, J.L., IEEE *Trans. Ultras. Ferr. Freq. Control*, 41 (1), 140-143 (1994).
2. Popovics, J.S., *Materials Evaluation*, 63 (1), 50-55 (2005).
3. Lafhaj, Z., Goueygou, M., Djerbi, A., Kaczmarek, *Cement and Concrete Research* 36(4), 625-633 (2006).
4. Lizzi F. L., Greenebaum M., Feleppa E. J., Elbaum M., Coleman, D. J., *J. Acoust. Soc. Am.*, 73(4), 1366-1373 (1983).
5. Insana M. F., Wagner R. F., Brown D. G., Hall T. J., *J. Acoust. Soc. Am.* 87(1), 179-192 (1990).
6. Oelze, M.L. and O'Brien Jr., W.D., *J. Acoust. Soc. Am.*, 111, 2308-2319, (2002).
7. Pao Y-H. and Mow C. C., *J. Appl. Phys.*, 34(3), 493-499 (1963).
8. Insana M. F. and Hall, T. J., *Ultras. Imag.* 12, 245-267 (1990).
9. Papadakis E.P., Fowler K.A., Lynnworth L.C., *J. Acoust. Soc. Am.*53(5), pp. 1336-1343 (1973).
10. Russ, J. C. and DeHoff, T., *Practical Stereology*, Kluwer Academic/Plenum, New York (2000).
11. Oelze, M.L. and O'Brien Jr., W.D., *Ultras. Imag.* 28, 83-96, (2006).

Downloaded 19 Jun 2009 to 130.126.119.40. Redistribution subject to AIP license or copyright; see http://proceedings.aip.org/proceedings/cpcr.jsp